REPUBLIC OF IRAQ

MINISTRY OF HIGHER EDUCATION AND

SCIENTIFIC RESEARCH

UNIVERSITY OF BABYLON

COLLEGE OF MATERIALS ENGINEERING

METAL DEPARTMENT

X-RAY DAFFRACTION POWDER (XRD) FOR ANAYLSIS OF Fe_2O_3 , Al_2O_3 NANO PARTICALS

PREPARE BY STUDENT:

ALI MUTHANNA AHMED

4TH YEAR

SUPERVISION OF

Dr: AYAD MOHAMED NATAH

2021/2022

بِسْمِ اللَّهِ الرَّحْمَنِ الرَّحِيمِ

(هُوَ الَّذِي بَعَثَ فِي الْأُمِّيِّينَ رَسُولًا مِّنْهُمْ يَتْلُو عَلَيْهِمْ آيَاتِهِ وَيُزَكِّيهِمْ وَيُعَلِّمُهُمُ الْكِتَابَ وَالْحِكْمَةَ وَإِن كَانُوا مِن قَبْلُ لَفِي ضَلَالٍ مُّبِينٍ)

صدق الله العلي العظيم

سورة الجمعة- الآية الثانية

الأهداء

الى اولياء نعمتي وأئمة الهدى محمد وآل محمد (ص) .....

الى نبراس الذي ينير دربي ... الى من اعطاني وما يزل يعطيني ... رفعت رأسي عالياً افتخاراً به...ابي العزيز ..... ادامه الله ذخراً لي .....

الى الذي رآني قلبها قبل عينها ... الى شجرتي التي لا تذبل .. امي الحبيبة .. حفظها الله

الى من هم سندي في حياتي من بعد الله عزوجل ..... اخوتي

الى كل من وقف بجانبي وكان لهما الفضل بعد الله فيما وصلت اليه ... اساتذتي ... اقربائي .....اصدقائي ...

اهدي جهدي المتواضع هذا .....

CONTENTS

CONTENTS

LIST OF TABLES

FIGUERS

THE THEORETICAL PART

X-ray

1- Historical Background

Before their discovery in 1895, X-rays were just a type of unidentified radiation emanating from experimental discharge tubes. They were noticed by scientists investigating cathode rays produced by such tubes, which are energetic electron beams that were first observed in 1869. Many of the early Crookes tubes (invented around 1875) undoubtedly radiated X-rays, because early researchers noticed effects that were attributable to them, as detailed below. Crookes tubes created free electrons by ionization of the residual air in the tube by a high DC voltage of anywhere between a few kilovolts and 100 kV as shown in figure 1. This voltage accelerated the electrons coming from the cathode to a high enough velocity that they created X-rays when they struck the anode or the glass wall of the tube.

Figure 1: Discharge tube of X-rays.

The earliest experimenter thought to have (unknowingly) produced X-rays was William Morgan. In 1785, he presented a paper to the Royal Society of London describing the effects of passing electrical currents through a partially evacuated glass tube, producing a glow created by X-rays. This work was further explored by Humphry Davy and his assistant Michael Faraday. When Stanford University physics professor Fernando Sanford created his "electric

photography", he also unknowingly generated and detected X-rays. From 1886 to 1888, he had studied in the Hermann von Helmholtz laboratory in Berlin, where he became familiar with the cathode rays generated in vacuum tubes when a voltage was applied across separate electrodes, as previously studied by Heinrich Hertz and Philipp Lenard. His letter of January 6, 1893 (describing his discovery as "electric photography") to The Physical Review was duly published and an article entitled Without Lens or Light, Photographs Taken With Plate and Object in Darkness appeared in the San Francisco Examiner.

Starting in 1888, Philipp Lenard conducted experiments to see whether cathode rays could pass out of the Crookes tube into the air. He built a Crookes tube with a "window" at the end made of thin aluminium, facing the cathode so the cathode rays would strike it (later called a "Lenard tube"). He found that something came through, that would expose photographic plates and cause fluorescence. He measured the penetrating power of these rays through various materials. It has been suggested that at least some of these "Lenard rays" were actually X-rays.

Helmholtz formulated mathematical equations for X-rays. He postulated a dispersion theory before Röntgen made his discovery and announcement. He based it on the electromagnetic theory of light.[full citation needed] However, he did not work with actual X-rays.

In 1894, Nikola Tesla noticed damaged film in his lab that seemed to be associated with Crookes tube experiments and began investigating this invisible, radiant energy. After Röntgen identified the X-ray, Tesla began making X-ray images of his own using high voltages and tubes of his own design, as well as Crookes tubes.

1.1 Importance of XRD

Measure the average spacings between layers or rows of atoms crystal or grain Determine the orientation of a single . Find the crystal structure of an unknown material. Measure the size, shape and internal stress of small crystalline regions.

1.2 X-ray Diffraction (XRD)

The atomic planes of a crystal cause an incident beam of X-rays to interfere with one another as they leave the crystal. The phenomenon is called X-ray diffraction as shown in figure 2.

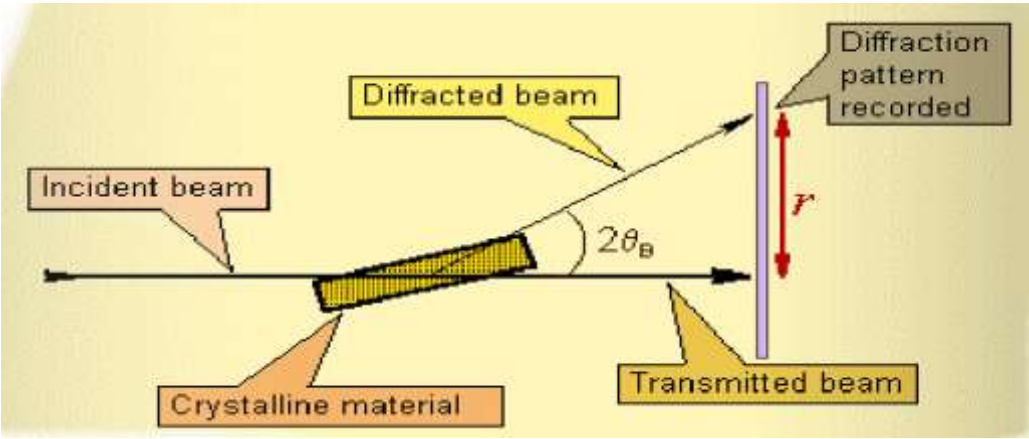

Figure 2: Principle work of X-ray diffraction .

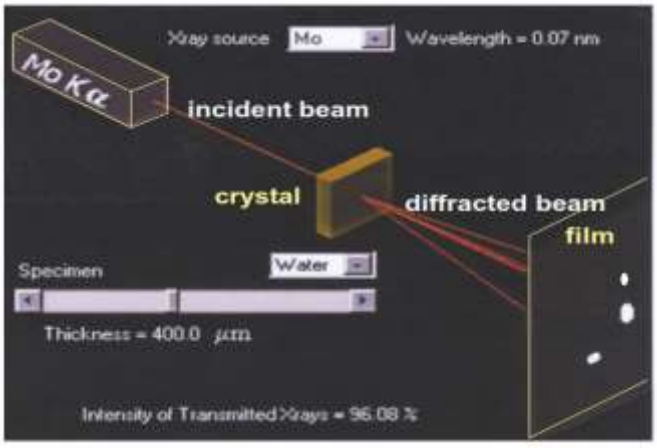

Figure 3: Effect of sample thickness on the absorption of x-rays.

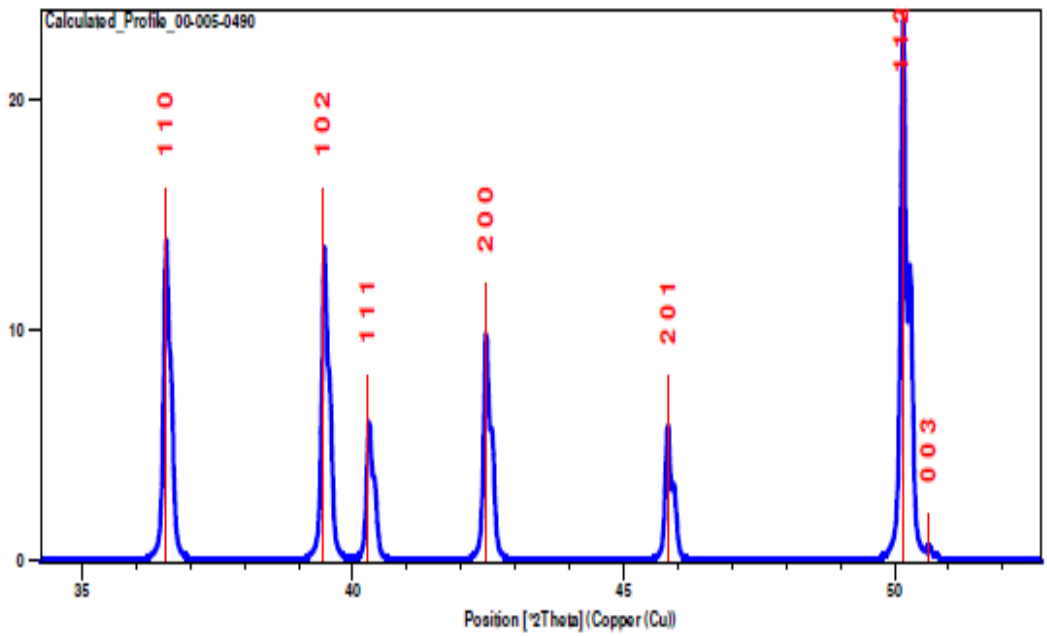

Figure 4: Diffraction peaks are associated with planes of atoms**.**

Miller indices (hkl) are used to identify different planes of atoms observed diffraction peaks can be related to planes of atoms to assist in analyzing the atomic structure and microstructure of a sample as shown in figure 5.

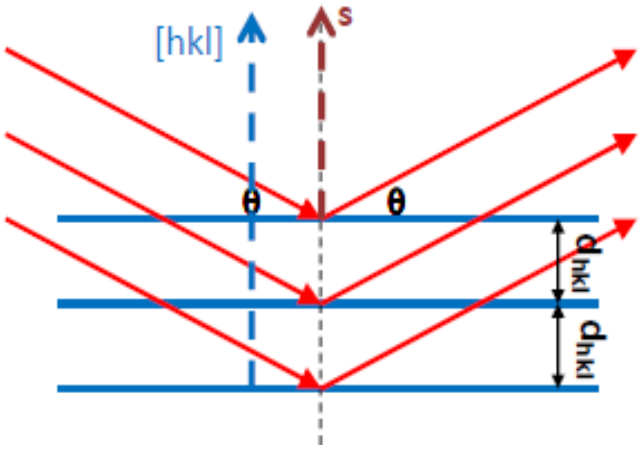

Figure 5: Miller indices for different peaks.

1.3 Bragg's Law

English physicists Sir W.H. Bragg and his son Sir W.L. Bragg developed a relationship in 1913 to explain why the cleavage faces of crystals appear to reflect X-ray beams at certain angles of incidence (theta, q). The variable d is the distance between atomic layers in a crystal, and the variable lambda l is the wavelength of the incident X-ray beam; n is an integer the formula of Bragg's Law is identify below.

$$\lambda = 2d_{hkl} \sin\theta$$

Bragg's law calculates the angle where constructive interference from X-rays scattered by parallel planes of atoms will produce a diffraction peak. Although Bragg's law was used to explain the interference pattern of X-rays scattered by crystals, diffraction has been developed to study the structure of all states of matter with any beam, e.g., ions, electrons, neutrons, and protons, with a wavelength similar to the distance between the atomic or molecular structures of interest.

XRD is a high-tech, non-destructive technique for analyzing a wide range of materials, including fluids, metals, minerals, polymers, catalysts, plastics, pharmaceuticals, thin film coatings, ceramics and semiconductors. Once the material has been identified, X-ray crystallography may be used to determine its structure, i.e. how the atoms pack together in the crystalline state and what the inter atomic distance and angle are etc. The detector moves in a circle around the sample.

The detector position is recorded as the angle 2theta (2θ). The detector records the number of X-rays observed at each angle 2θ -The X-ray intensity is usually recorded as "counts" or as "counts per second. Many powder diffracto meters use the Bragg-Brentano parafocusing Geometry. To keep the

X-ray beam properly focused, the incident angle omega changes in conjunction with 2 theta. This can be accomplished by rotating the sample or by rotating the X-ray tube . The X-ray diffraction test as shown in Figure 6.

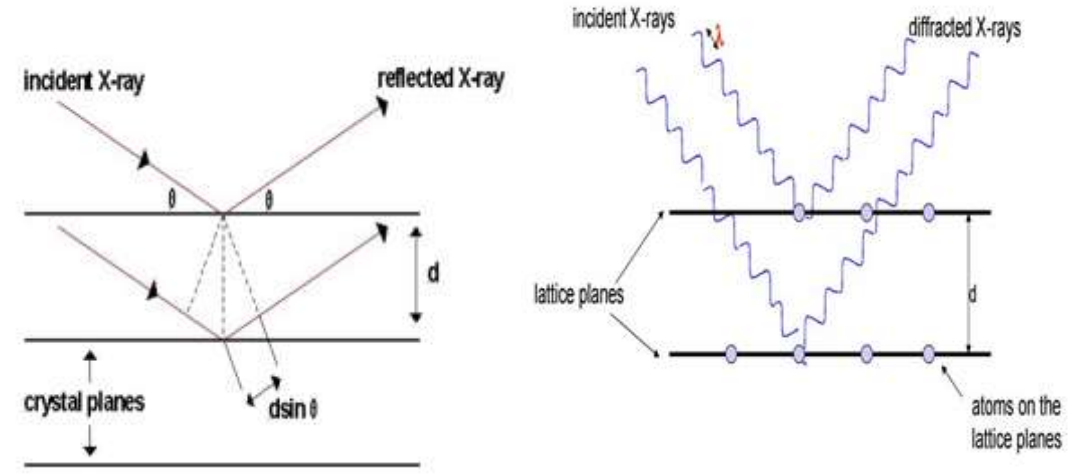

(a)

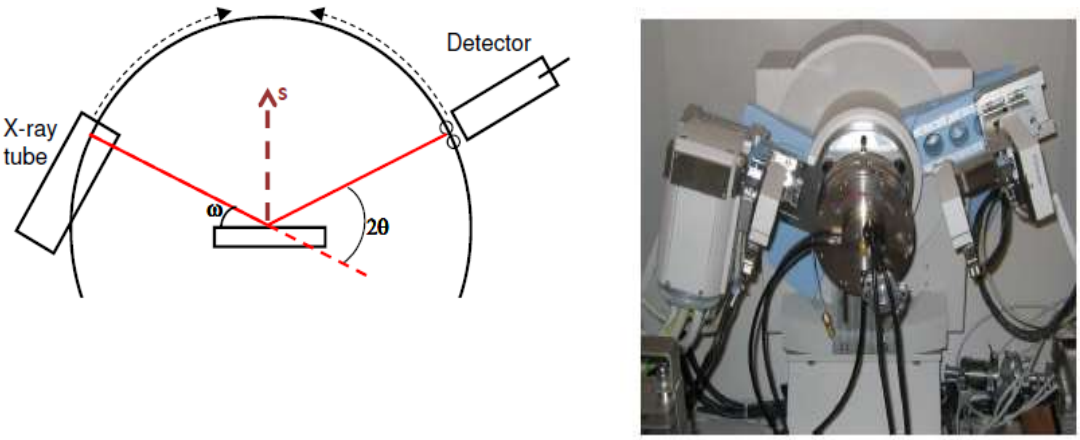

(b)

Figure 6 : A schematic of X-Ray diffraction beam (a) principles of work X-ray powder diffraction (b) .

1.4 Diffraction Basics

For electromagnetic radiation to be diffracted the spacing in the grating. should be of the same order as the wavelength. In crystals the typical interatomic spacing ~ 2-3 Å so the suitable radiation is X –rays Hence, X-

rays can be used for the study of crystal structures Neutrons and Electrons are also used for diffraction studies from materials. Neutron diffraction is especially useful for studying the magnetic ordering in materials see figure 7.

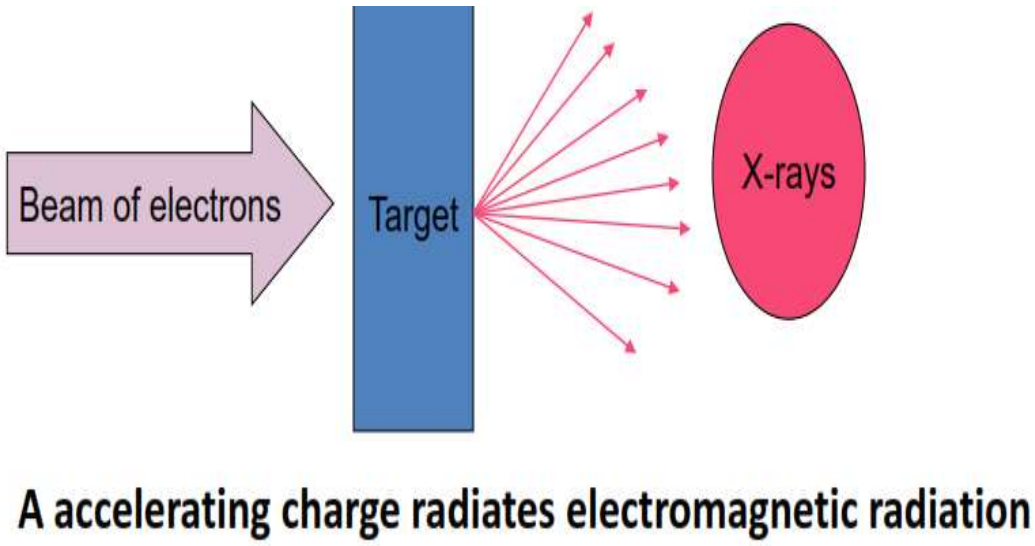

Figure 7: An X-ray powder diffraction pattern is a plot of the intensity of X-rays scattered at different angles by a sample.

2. Measurements of nanoparticle phase using XRD technique

X-Ray power diffraction method was used in the present work to determine the nanoparticle crystalline structure. X-ray power diffraction method (XRD) has now become one of the most widely-used techniques and can be engaged to study the structure and microstructure of crystalline solids. It is also considered as a routine method engaged by solid-state chemists and mineralogists. XRD was used extensively by researchers such as Memon et al. Figure 6 (a) shows the incidence and reflection of the X-ray on the plane with their angle. The main components of the XRD instrument include a sample holder, X-ray tube, and an X-ray detector. The mechanism process of XRD is based on X-rays that are generated by the X-ray tube to produce electrons which are located on the left as the source. The sample is placed in the middle

and the electrons as diffracted rays fall on the detector on the right. The X-ray tube rotates clockwise by angle θ whereas the detector rotated by angle 2θ. The clockwise rotation for the X-ray tube allows for the X-ray beam to focus on the sample. The number of X-rays observed at each angle can be recorded by moving the X-ray detector around the sample. The 2θ plot can be obtained where there are peaks corresponding to diffraction from the different planes in the polycrystalline material - see Figure 6 (b).

2.1. Determination of nanoparticle size from XRD spectra

The mean particle size measurements between XRD and STEM are highly important. It can be seen that the size of the nanoparticle which was measured by the XRD technique is less than that from the STEM technique. This is because the STEM is mainly focused on the primary single particles, whereas the XRD is focused on the bulk material purity and crystal lines. The most common and simplest method for calculating the average crystallite size is from the full width at half maximum (FWHM) of a diffraction peak by using the Scherrer equation 1 as follows:

$$d_{XRD} = \frac{K\lambda}{B \cos\theta} \quad \textbf{(nm)} \quad \textbf{……1}$$

Where d= the crystallite size, and K = Scherrer constant in the formula accounts for the particle shape of value 0.9. B = is the corrected FWHM, λ = wavelength of x-rays, and θ = is the Bragg or diffraction angle of x-rays . Also, the crystal lattice planes of the nanoparticles can be calculated by using Bragg's Law as shown in equation 2:

$$\mathbf{n\lambda = 2\ d\ Sin\ \theta} \quad \textbf{…….2}$$

Where λ is the wavelength of the x-rays, n is an integer, d is the spacing between two atomic layers, and θ is the angle between the incoming x-ray and the atom layer . The phase and particle size of iron oxide nanoparticles can also be determined with an x-ray diffractometer by using the Scherrer formula.

3. Nanomaterials

3.1 Nanoparticles- types, classification and applications

The nanoparticles in nanotechnology science, is defined as a small object that behaves as a whole unit in terms of its transport and properties. They play an important role in a wide variety of fields including advanced materials, pharmaceuticals, and environmental detection and monitoring. Therefore, nanoparticles have been employed in various important areas, opening doors for new advancement in different fields and making a significant contribution to modern science .

Typically, nanoparticles can be classified according to their dimensionality, morphology, composition, uniformity, and agglomeration. Nano-sized particles with diameter less than 10 nm are of explicit interest because of the physical and chemical behaviour of these particles arising from the quantum size effect that is significantly different from their bulk form .

Morphology and distribution of particle size plays an important role related to the parameters of the characterisation of nanoparticles . Morphological characteristics to be considered are: flatness, sphericity, and aspect ratio, as shown in Figure 8.

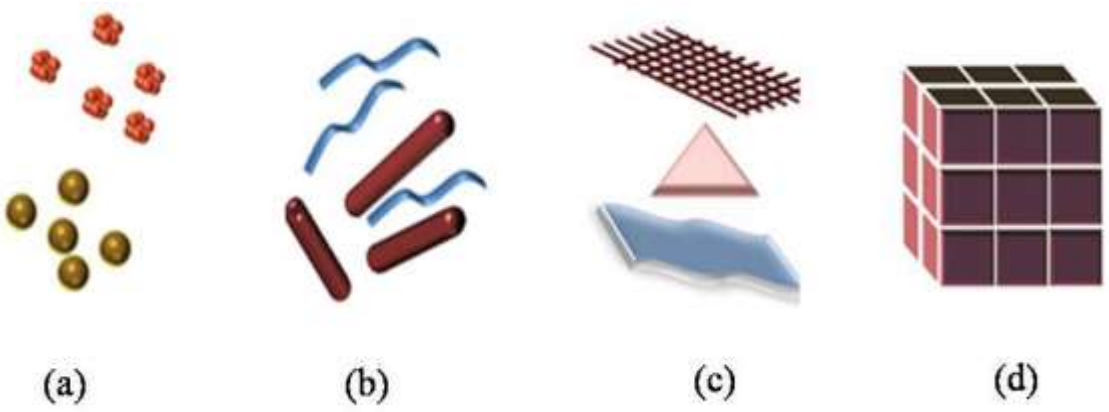

Figure 8: Classification of nanomaterials (a) 0D spheres and clusters, (b) 1D nanofibres, wires, and rods, (c) 2D films, plates, and networks, (d) 3D nanomaterials .

Classification of nanomaterials depends on their dimension, nanoparticles are divided into one, two and three dimensional . There are five main categories of nanoparticle which can be classified into the following types: Fullerenes, Carbon Nanotubes, Metals, Ceramics, Semiconductors (Quantum dots) and Polymerics.

There are different metal oxides namely gold, silver, copper, alloy and iron which have been attracted a great deal of interest due to their potential applications in nanoscience.

3.2 Application of nanoparticles

Nanoscale particles have attracted considerable attention due to their potential properties. Therefore, the small size of nanoparticles smaller than 100 nm directly influences different properties that will be more suitable for new applications. Nanoparticles are used for various applications such as electronic, chemical and mechanical, as well as in the related technologies using catalysts, pigments, drug carriers, sensors, and in electronic magnetic

materials . Table 1 shows the range of applications of nanoparticles in the various practical areas.

Table 1: Application of nanotechnology in different fields .

Applied field	Application
Materials	Nanoparticles, carbon nanotubes, biopolymers, paints, coatings
Electronics	Semiconductor chips, memory storage, photonic, optoelectronics
Scientific Tools	Atomic force, microscopic and scanning tunneling microscope
Food Sciences Environment and Energy	Processing, nutraceutical food, nanocapsules. Water and air purification filters, fuel cells, photovoltaic
Chemical and Cosmetics	Nanoscale chemicals and compounds, paints, coatings etc.
Nanomedicines	Nano drugs, medical devices, tissue engineering

In recent years, iron oxide nanoparticles have attracted more interest due to their unique optical, electrical and magnetic properties. This is preferable for many potential applications such as magnetic storage media, pigments and development of gas sensors, as well as electronic and optical devices, information storage, and wastewater treatment adsorbents . Over the last few years, pollution from heavy metals has become one of the most serious environmental problems. Therefore, considerable attention has been focused on removal of heavy metals from contaminated water via an absorption process. It is found that nanoparticles are efficient as absorbents for removal of heavy metals such as Pb^{+2} from industrial wastewater. For example, γ-Fe_2O_3 nanoparticles with particle size of 60 nm have a significant effect due to

their distinctive properties such as large area-to-volume ratio . The use of nanoparticles to catalyze reactions has undertaken an explosive growth during the past decade and includes homogeneous and heterogeneous catalysis.

Nanoparticles provide unique properties due to their high surface area to volume ratio compared to bulk materials. Thus, they are more attractive to use for catalysis; typically, with small particles size (10-80 nm). Nanoparticles were studied as significant and potential gas sensing materials because of their optical properties including band gap energy and absorbance. Thus, nanoparticles are potentially and widely used as sensing layers for different types of gas sensor. Nanoparticles have also had a significant role in and can be successfully used on planar solar cell substrates. The configuration of the assembled DSSCs with magnetic γ-Fe_2O_3 NPs is shown schematically in Figure 9.

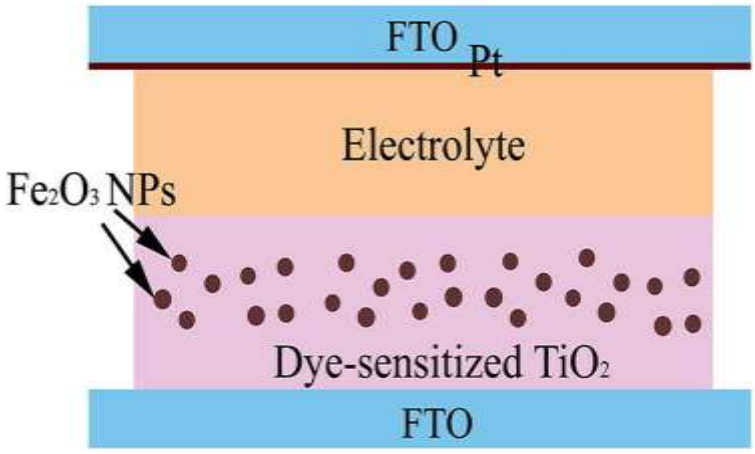

Figure 9: Schematic of dye-sensitised solar cells with γ-Fe_2O_3 nanoparticle.

4. Aluminium oxide

Aluminium oxide is a chemical compound of aluminium and oxygen with the chemical formula Al_2O_3. It is the most commonly occurring of several aluminium oxides, and specifically identified as aluminium(III) oxide. It is

commonly called alumina and may also be called aloxide, aloxite, or alundum depending on particular forms or applications as shown in figure 10. It occurs naturally in its crystalline polymorphic phase α-Al_2O_3 as the mineral corundum, varieties of which form the precious gemstones ruby and sapphire. Al_2O_3 is significant in its use to produce aluminium metal, as an abrasive owing to its hardness, and as a refractory material owing to its high melting point.

Figure 10: Powder of aluminum oxide**.**

4.1 Natural occurrence

Corundum is the most common naturally occurring crystalline form of aluminium oxide. Rubies and sapphires are gem-quality forms of corundum, which owe their characteristic colours to trace impurities. Rubies are given their characteristic deep red colour and their laser qualities by traces of chromium. Sapphires come in different colours given by various other impurities, such as iron and titanium. An extremely rare, δ form, occurs as the mineral deltalumite.

4.2 Properties

Al_2O_3 is an electrical insulator but has a relatively high thermal conductivity (30 Wm−1K−1) for a ceramic material. Aluminium oxide is insoluble in water. In its most commonly occurring crystalline form, called corundum or α-aluminium oxide, its hardness makes it suitable for use as an abrasive and as a component in cutting tools.

Aluminium oxide is responsible for the resistance of metallic aluminium to weathering. Metallic aluminium is very reactive with atmospheric oxygen, and a thin passivation layer of aluminium oxide (4 nm thickness) forms on any exposed aluminium surface in a matter of hundreds of picoseconds. This layer protects the metal from further oxidation. The thickness and properties of this oxide layer can be enhanced using a process called anodising. A number of alloys, such as aluminium bronzes, exploit this property by including a proportion of aluminium in the alloy to enhance corrosion resistance. The aluminium oxide generated by anodising is typically amorphous, but discharge assisted oxidation processes such as plasma electrolytic oxidation result in a significant proportion of crystalline aluminium oxide in the coating, enhancing its hardness. Aluminium oxide was taken off the United States Environmental Protection Agency's chemicals lists in 1988. Aluminium oxide is on the EPA's Toxics Release Inventory list if it is a fibrous form.

4.3 Structure

The most common form of crystalline aluminium oxide is known as corundum, which is the thermodynamically stable form. The oxygen ions form a nearly hexagonal close-packed structure with the aluminium ions filling two-thirds of the octahedral interstices. Each Al_3+ center is octahedral. In terms of its crystallography, corundum adopts a trigonal Bravais lattice

with a space group of R3c (number 167 in the International Tables). The primitive cell contains two formula units of aluminium oxide.

Aluminium oxide also exists in other metastable phases, including the cubic γ and η phases, the monoclinic θ phase, the hexagonal χ phase, the orthorhombic κ phase and the δ phase that can be tetragonal or orthorhombic. Each has a unique crystal structure and properties. Cubic γ-Al_2O_3 has important technical applications. The so-called β-Al_2O_3 proved to be NaAl11O17.

Molten aluminium oxide near the melting temperature is roughly 2/3 tetrahedral (i.e. 2/3 of the Al are surrounded by 4 oxygen neighbors), and 1/3 5-coordinated, with very little (<5%) octahedral Al-O present. Around 80% of the oxygen atoms are shared among three or more Al-O polyhedra, and the majority of inter-polyhedral connections are corner-sharing, with the remaining 10–20% being edge-sharing. The breakdown of octahedra upon melting is accompanied by a relatively large volume increase (~33%), the density of the liquid close to its melting point is 2.93 g/cm^3. The structure of molten alumina is temperature dependent and the fraction of 5- and 6-fold aluminium increases during cooling (and supercooling), at the expense of tetrahedral AlO_4 units, approaching the local structural arrangements found in amorphous alumina.

4.4 Applications

Known as alpha alumina in materials science communities or alundum (in fused form) or aloxite in the mining and ceramic communities aluminium oxide finds wide use. Annual world production of aluminium oxide in 2015 was approximately 115 million tonnes, over 90% of which is used in the manufacture of aluminium metal. The major uses of speciality aluminium oxides are in refractories, ceramics, polishing and abrasive applications. Large

tonnages of aluminium hydroxide, from which alumina is derived, are used in the manufacture of zeolites, coating titania pigments, and as a fire retardant/smoke suppressant.

Over 90% of the aluminium oxide, normally termed Smelter Grade Alumina (SGA), produced is consumed for the production of aluminium, usually by the Hall–Héroult process. The remainder, normally called speciality alumina is used in a wide variety of applications which reflect its inertness, temperature resistance and electrical resistance.

4.5 Abrasion protection

Aluminium oxide can be grown as a coating on aluminium by anodizing or by plasma electrolytic oxidation (see the "Properties" above). Both the hardness and abrasion-resistant characteristics of the coating originate from the high strength of aluminium oxide, yet the porous coating layer produced with conventional direct current anodizing procedures is within a 60–70 Rockwell hardness C range which is comparable only to hardened carbon steel alloys, but considerably inferior to the hardness of natural and synthetic corundum. Instead, with plasma electrolytic oxidation, the coating is porous only on the surface oxide layer while the lower oxide layers are much more compact than with standard DC anodizing procedures and present a higher crystallinity due to the oxide layers being remelted and densified to obtain α-Al_2O_3 clusters with much higher coating hardness values circa 2000 Vickers hardness.

Alumina is used to manufacture tiles which are attached inside pulverized fuel lines and flue gas ducting on coal fired power stations to protect high wear areas. They are not suitable for areas with high impact forces as these tiles are brittle and susceptible to breakage.

5. Iron oxide

Iron(III) oxide or ferric oxide is the inorganic compound with the formula Fe_2O_3. It is one of the three main oxides of iron, the other two being iron(II) oxide (FeO), which is rare; and iron(II,III) oxide (Fe_3O_4), which also occurs naturally as the mineral magnetite. As the mineral known as hematite, Fe_2O_3 is the main source of iron for the steel industry. Fe_2O_3 is readily attacked by acids. Iron(III) oxide is often called rust, and to some extent this label is useful, because rust shares several properties and has a similar composition; however, in chemistry, rust is considered an ill-defined material, described as Hydrous ferric oxide.

5.1 Importance, structure and properties of Fe_2O_3 nanoparticles.

Ferric oxide (Fe_2O_3) is a transition metal oxide nanoparticle with unique scientific and technological importance due to its size dependent physical–chemical properties and its excellent applications in different areas such as electronics, catalysis, gas detection, energy storage and magnetic resonance imaging .The properties of hematite Fe_2O_3 are highly influenced by their particle size, morphology, and their structure whereas, the maghemite Fe_2O_3 is one of the most important materials effectively used in biomaterials because of their biocompatibility. The three iron-oxide have different crystal structures based on close - packed planes of iron cations with oxygen ions. Magnetite and maghemite have the same crystal structure. In maghemite the oxygen ions are arranged in a cubic close- packed array. Whereas, in hematite, oxygen ions are arranged in a hexagonal close-packed array and Fe (III) ions occupy octahedral sites. The crystal structures are shown in Figure 11.

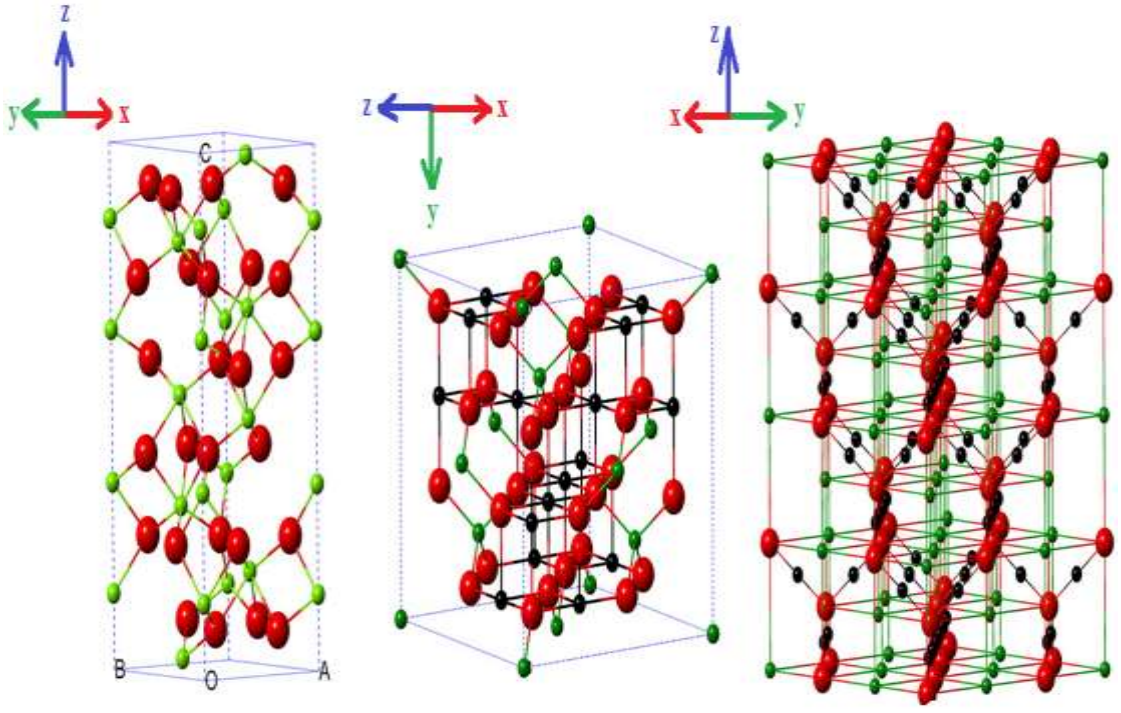

(a) **(b)** **(c)**

Figure 11: Phase structures of (a) hematite, (b) magnetite and (c) maghemite.

Experimental Part

There are two types of nanomaterials, iron oxide Fe_2O_3 and alumina AL_2O_3 , were used in this project and were examined with an X-ray machine (XRD) as shown in figure 12.

Figure 12: The XRD operation machine**.**

Action Steps

1- Sample preparation process: By placing the powder to be examined in the x-ray in its designated place to be placed inside the machineThe picture below shows the place designated for placing the powder (sample).

2-Sample inspection process: After completing the sample preparation process, we install the sample in the machine, and then the sample is examined as in the picture below.

3- Screening analysis process: After performing the two previous operations, we analyze the results of the examination for alumina Al_2O_3 and iron oxide Fe_2O_3, and they are compared with the approved standards to match the results of the examination analysis as shown below and the XRD plot and reference plots are in good agreement..

3.1 Iron oxide Fe_2O_3

Figure 13: shows the XRD pattern phase of tested powder of the Fe_2O_3 nanoparticles that tested by X-ray Powder Diffraction (XRD) .

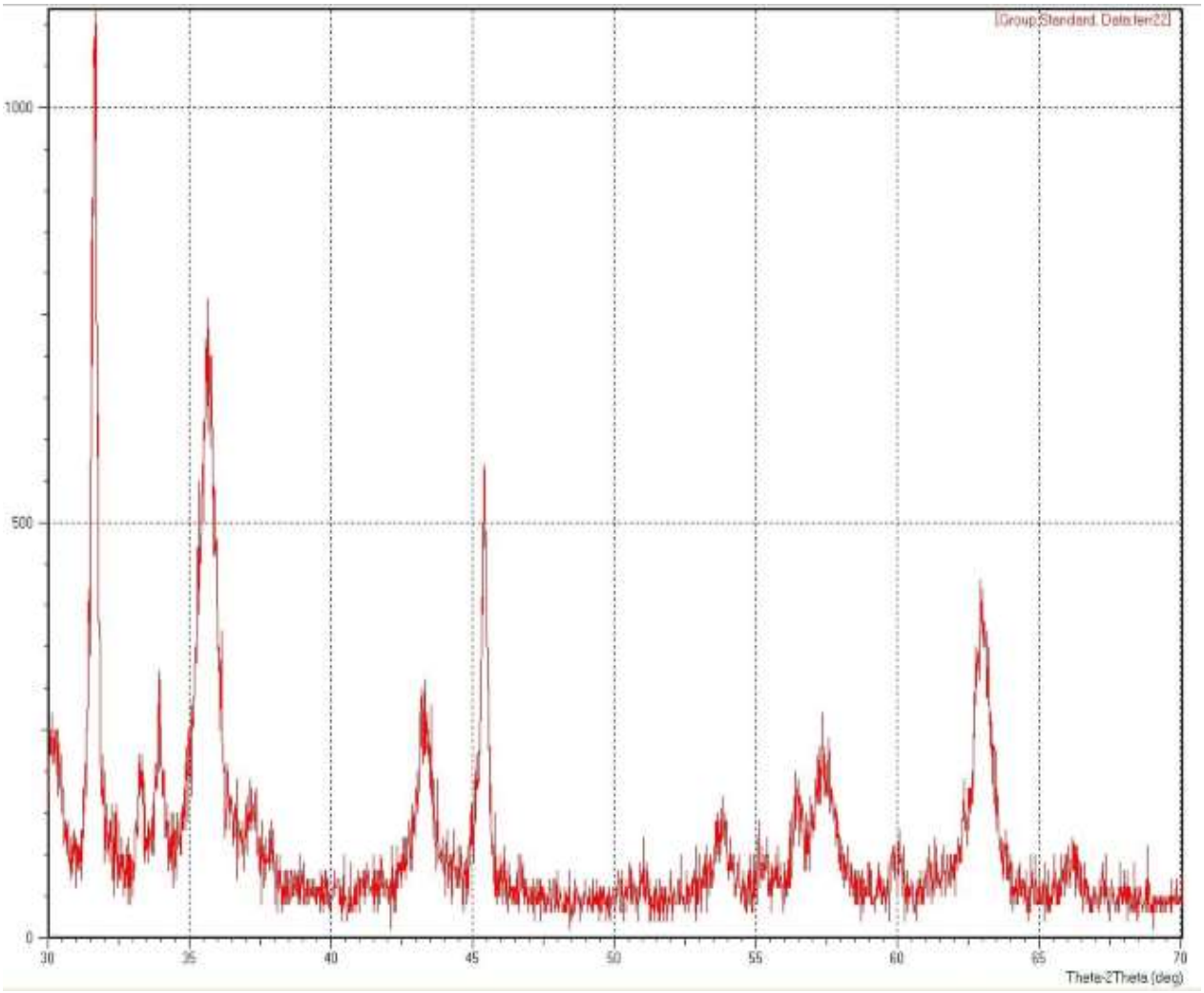

Figure 13: Scheme showing the assay analysis of iron oxide nanoparticles by X-ray .

Figure 14: shows the XRD pattern phase of standard samples of the Fe_2O_3 nanoparticles prepared and tested by X-ray Powder Diffraction (XRD) .

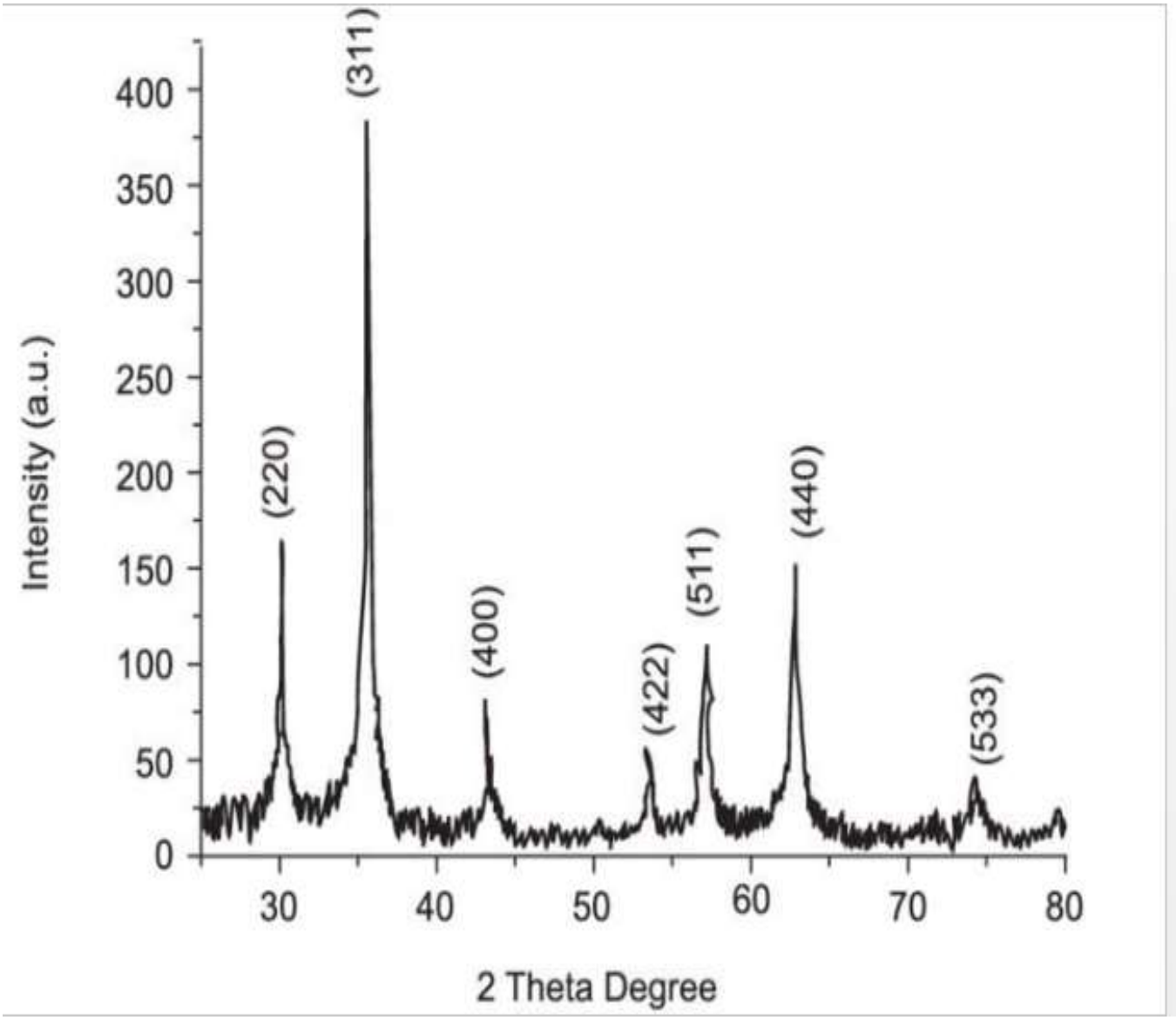

Figure 14: Iron oxide Fe_2O_3 standard peak.

3.2 Alumina Al_2O_3

Figure 15: shows the XRD pattern phase of standard samples of the Al_2O_3 nanoparticles that tested by X-ray Powder Diffraction (XRD) .

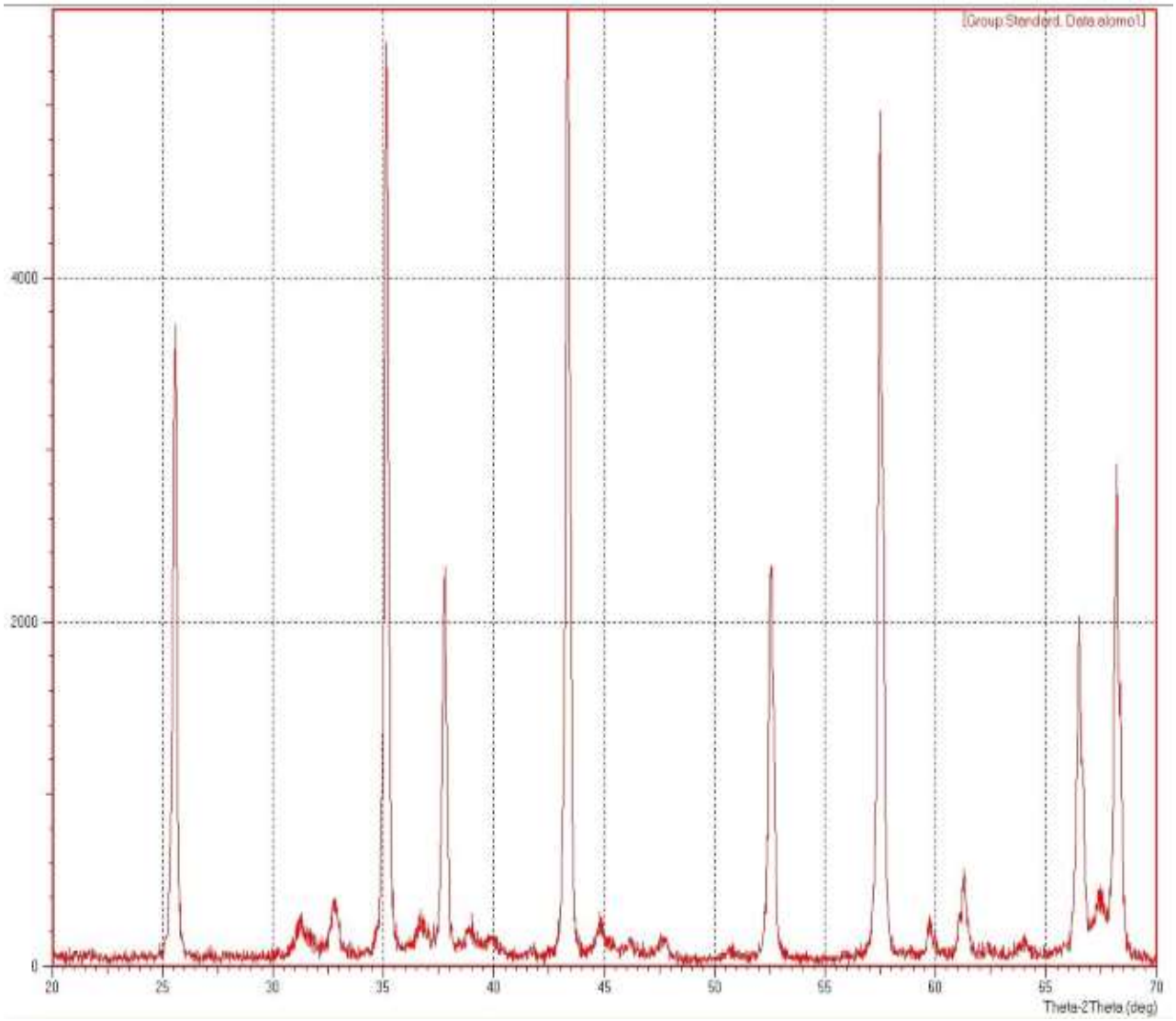

Figure 15: Scheme showing the analysis of the results of X-ray alumina nanoparticles.

Figure 16 : shows the XRD pattern phase of standard samples of the Al_2O_3 nanoparticles prepared and tested by X-ray Powder Diffraction (XRD).

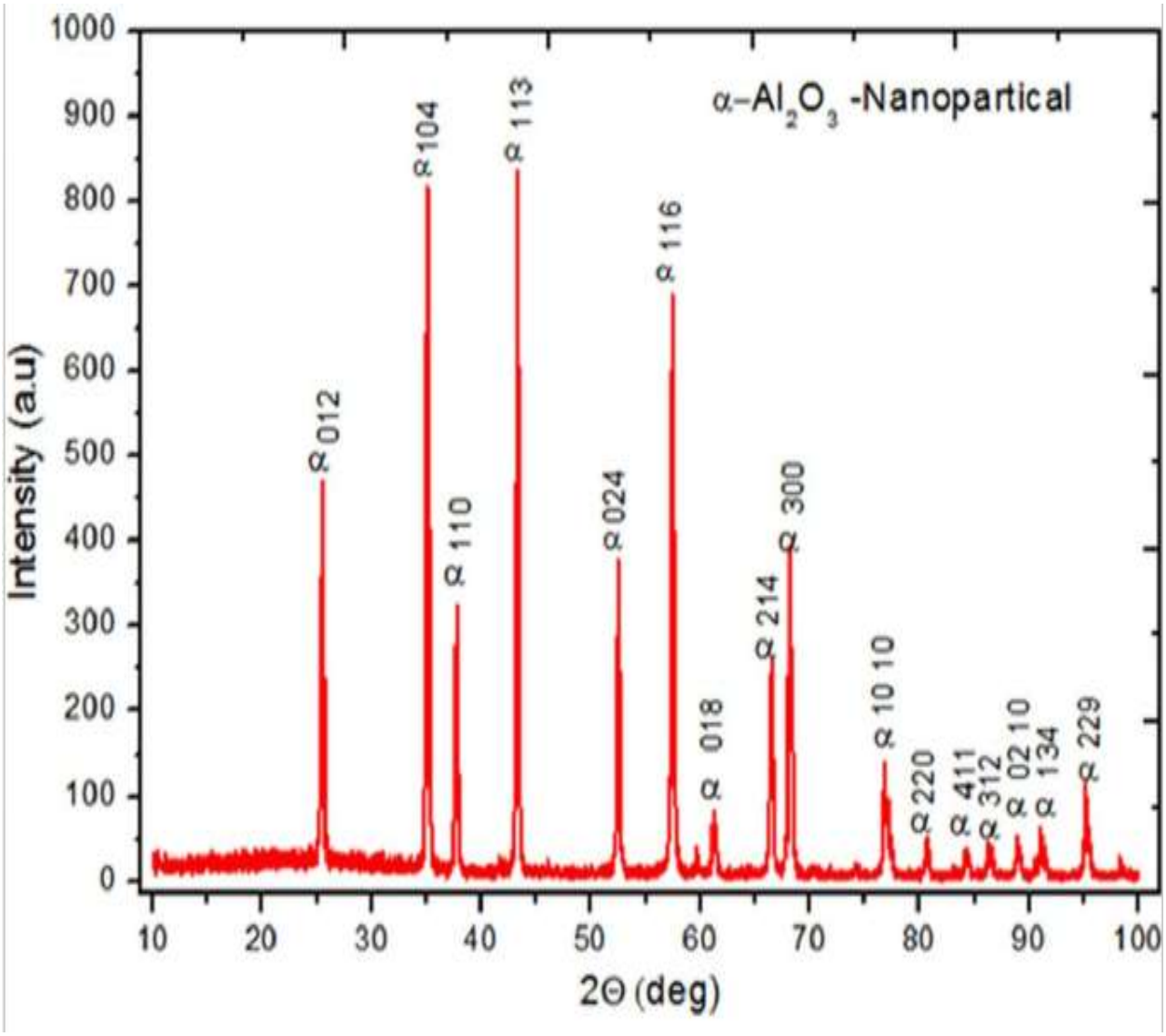

Figure 16: Alumina Al_2O_3 standard peak.

References:

"Aloxite". ChemIndustry.com database. Archived from the original on 25 June 2007. Retrieved 24 February 2007.

"Alumina (Aluminium Oxide) – The Different Types of Commercially Available Grades". The A to Z of Materials. 3 May 2002. Archived from the original on 10 October 2007. Retrieved 27 October 2007.

"Deltalumite" "EPCRA Section 313 Chemical List For Reporting Year 2006" (PDF). US EPA. Archived from the original (PDF) on 2008-05-22. Retrieved 2008-09-30.

"List of Minerals". 21 March 2011.

Chadda, P. K. (2009). Hydroenergy and Its Energy Potential. Pinnacle Technology. p. 88.

Anderson, J.G. (January 1945), "William Morgan and X-rays", Transactions of the Faculty of Actuaries.

B. Sun, J. Horvat, H. S. Kim, W.-S. Kim, J. Ahn, and G. Wang, Synthesis of mesoporous α-Fe_2O_3 nanostructures for highly sensitive gas sensors and high capacity anode materials in lithium ion batteries, Journal of Physical Chemistry C, vol. 114, no. 44, 2010, pp. 18753–18761.

Buzea, Cristina; Pacheco, Ivan; Robbie, Kevin (2007). "Nanomaterials and Nanoparticles: Sources and Toxicity". Biointerphases. 2 (4): MR17–MR71 .

C. Buzea, I. Pacheco, K. Robbie, Nanomaterials and Nanoparticles: Sources and Toxicity. *Biointerphases* Vol. 2, 2007, pp. MR17.

Elam, J. W. (October 2010). Atomic Layer Deposition Applications 6. The Electrochemical Society.

F. CAI, S. Zhang, and Z. Yuan, Effect of magnetic gamma-iron oxide nanoparticles on the efficiency of dye-sensitized solar cells. The Royal Society of Chemistry, RSC Advance. 5, 2015, 42869–42874.

Filler, Aaron (2009). "The History, Development and Impact of Computed Imaging in Neurological Diagnosis and Neurosurgery: CT, MRI, and DTI". Nature Precedings.

H. Xu, X. Wang, L. Zhang, Selective preparation of nanorods and micro-octahedrons of Fe_2O_3 and their catalytic performances for thermal decomposition of ammonium perchlorate. Powder Technology 185, 2008, 176–180.

Hrabak, M.; Padovan, R. S.; Kralik, M.; Ozretic, D.; Potocki, K. (July 2008). "Nikola Tesla and the Discovery of X-rays". RadioGraphics. 28 (4): 1189–92.

Hubler, A.; Osuagwu, O. (2010). "Digital quantum batteries: Energy and information storage in nanovacuum tube arrays". Complexity: NA.

K. Okuyama, and W. Lenggoro, Nanoparticle Preparation and Its Application - A Nanotechnology Particle Project in Japan, Computer Society. 2004, pp.1-4.

K.K. Balasubramanian, M. Burghard, Chemically functionalized carbon nanotubes. Small, 1, No.2, 2005, 180–192.

M. Abhilash, Potential applications of Nanoparticles. International Journal of Pharma and Bio Sciences V1 (1), 2010.

M. Shahmiri, N. A. Ibrahim, N. Zainuddin, N. Asim, B. Bakhtyar, A. Zaharim, and K. Sopian, “Effect of pH on the synthesis of CuO nanosheets by quick precipitation method,” Wseas Transactions on Environmental and Development, Vol. 9, 2013.

M.M. Rahman, S. B. Khan, A. Jamal, M. Faisal, and A.M. Aisiri, Iron Oxide Nanoparticles. Department of Chemistry, Nanomaterials, Prof. Mohammed Rahman (Ed.), 2011. InTech, Available from: http://www.intechopen.com/books/nanomaterials/iron-oxide-nanoparticles.

McGovern, C. (2010). "Commoditization of nanomaterials". Nanotechnol. Perceptions. 6 (3): 155–178.

Morgan, William (1785-02-24). "Electrical Experiments Made in Order to Ascertain the Non-Conducting Power of a Perfect Vacuum, &c". Philosophical Transactions of the Royal Society. Royal Society of London.

Portela, Carlos M.; Vidyasagar, A.; Krödel, Sebastian; Weissenbach, Tamara; Yee, Daryl W.; Greer, Julia R.; Kochmann, Dennis M. (2020). "Extreme mechanical resilience of self-assembled nanolabyrinthine materials". Proceedings of the National Academy of Sciences. 117 (11)3.

R. Zboril, M. Mashlan, and D. Petridis, Iron (III) Oxides from Thermal Processes: Synthesis, Structural and Magnetic Properties, Mossbauer

Spectroscopy Characterization, and Applications, Chemistry of Materials, 14(3), 2002, 969-982.

S. Chaturvedi, P.N. Dave, N.K. Shah, Applications of nano-catalyst in new era. Journal of Saudi Chemical Society 16, 2012, 307–325.

S.L. Pal, U. Jana, P.K. Manna, G.P. Mohanta, R. Manavalan, Nanoparticle: An overview of preparation and characterization, Journal of Applied Pharmaceutical Science, 01 (06), 2011, pp. 228-234. [Online]. Available at: www.japsonline.com.

Sadri, Rad (1 January 2018). "A facile, bio-based, novel approach for synthesis of covalently functionalized graphene nanoplatelet nano-coolants toward improved thermo-physical and heat transfer properties". Journal of Colloid and Interface Science. 509: 140–152.

Thomson, Joseph J. (1903). The Discharge of Electricity through Gasses. USA: Charles Scribner's Sons. pp. 182–186.

W. Wu, Z. Wu, T. Yu, C. Jiang, and W.S. Kim, Recent progress on magnetic iron oxide nanoparticles: synthesis, surface functional strategies and biomedical applications. Sci. Technol. Adv. Mater. 16, 2015, 023501, pp.43.
Wiedmann's Annalen, Vol. XLVIII

Wyman, Thomas (Spring 2005). "Fernando Sanford and the Discovery of X-rays". "Imprint", from the Associates of the Stanford University Libraries: 5–15.

Z. Cheng, A.L. K Tan, Y. Tao, D. Shan, K.E. Ting, X.J. Yin, Synthesis and characterization of iron oxide nanoparticles and applications in the removal of heavy metals from industrial wastewater. International Journal of Photoenergy, 2012.